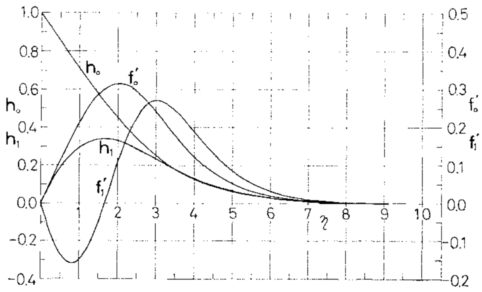

Fig. 1 The functions f'_0, f'_1, h_0, and h_1.

where the primes denote differentiation with respect to η. It should be noted that Eq. (8a) coincides with the governing equation for the laminar wall jet over an impermeable surface, the solution of which is plotted by Glauert.[2] Once f_0 is known, it is an easy matter to solve Eq. (8b) numerically. It thus remains to solve Eqs. (8c) and (8d), and the results will provide the first-order effects of the blowing or suction on the wall jet and the heat transfer. Corresponding to the boundary conditions given by Eqs. (4) and (5), the functions f and h take the following boundary values:

$$\eta = 0: \quad f_0 = f'_0 = 0, h_0 = 1$$

$$f_1 = -1/[2(n+1)], f'_1 = h_1 = 0$$

$$\eta = \infty: \quad f'_0 = h_0 = 0, f'_1 = h_1 = 0$$

By utilizing the Runge-Kutta-Gill method, the solutions of Eqs. (8c) and (8d) were obtained numerically for $P_r = 0.72$ and $n = 0$ on HIPAC 103 electronic digital computer installed at the Computer Center of Hokkaido University. The calculated results are tabulated in Table 1, together with the values of $f''_0(0)$ and $h'_0(0)$ that were used as the input data for Eqs. (8c) and (8d). The information contained in Table 1 will be used in the skin-friction and heat-transfer calculations which follow. Additionally, the functions f'_0, f'_1 and h_0, h_1, respectively, related to the velocity and temperature profiles, are plotted in Fig. 1.

Skin Friction and Heat Transfer

The skin friction τ may be calculated from $\tau(x) = (\partial u/\partial y)_{y=0}$. Introducing the variables ξ and η, the skin friction takes the form

$$\tau(x)/\tau_0(x) = 1 + [f''_1(0)/f''_0(0)]\xi + \ldots$$
$$= 1 - 1.72494(v_w x^{(3/4)}) + \ldots \qquad (9)$$

where $\tau_0(x)$ is the skin friction when suction or blowing is absent. Equation (9) provides the expected result that blowing decreases the skin friction, while suction increases the skin friction.

The local heat transfer $q(x)$ passing per unit area from the surface to the fluid can be evaluated by Fourier's law. In the same way as the skin friction, one obtains the expression

$$q(x)/q_0(x) = 1 + [h'_1(0)/h'_0(0)]\xi + \ldots$$
$$= 1 - 1.55618(v_w x^{(3/4)}) + \ldots \qquad (10)$$

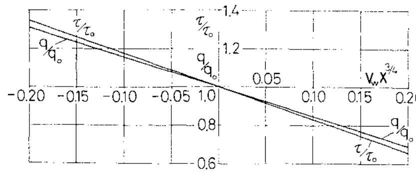

Fig. 2 Effect of blowing and suction on local skin friction and local heat transfer.

Table 1 Velocity and temperature derivatives

$f''_0(0)$	$f''_1(0)$	$h'_0(0)$	$h'_1(0)$
0.22222	−0.38332	−0.28676	0.44625

in which $q_0(x)$ represents the heat-transfer rate for the case of an isothermal, impermeable wall. Corresponding to the skin-friction case, blowing decreases the heat transfer, while suction increases the heat transfer. To facilitate interpretation of the results, Eqs. (9) and (10) have been plotted in Fig. 2.

Discussion of Results

To obtain perspective as to the magnitude of the blowing and suction velocities involved, one may use as a reference quantity the maximum velocity u_{max} corresponding to an isothermal impermeable wall, as was done by Sparrow and Cess[3] in the case of free convection due to a heated vertical flat plate with blowing and suction at the surface. From Glauert,[2] u_{max} is given by

$$u_{max} = 0.315x^{-(1/2)}$$

By the use of this relation and the expression for ξ with $n = 0$, it is easy to show that

$$v_w/u_{max} = 3.18x^{-(1/4)}\xi$$

Suppose one considers an abscissa value of ± 0.1, which corresponding to a 17% change in skin friction and a 16% change in heat transfer, respectively. Then, $v_w/u_{max} = 0.318x^{-1/4}$. For a current length of 10^4, $v_w/u_{max} = 0.0318$; while when $x = 10^6$, $v_w/u_{max} = 0.0100$. It is thus demonstrated that very small blowing and suction velocities can significantly effect the skin friction and heat transfer.

References

[1] Fox, H. and Steiger, M. H., "Some Mass Transfer Effects on the Wall Jet," *Journal of Fluid Mechanics*, Vol. 15, 1963, pp. 597–609.

[2] Glauert, M. B., "The Wall Jet," *Journal of Fluid Mechanics*, Vol. 1, 1956, pp. 625–643.

[3] Sparrow, E. M. and Cess, R. D., "Free Convection with Blowing or Suction," *Transactions of the ASME, Ser. C: Journal of Heat Transfer*, Vol. 83, pp. 387–389.

Spin Decay of Explorer XX

P. C. Hughes* and D. B. Cherchas†
University of Toronto, Toronto, Canada

THE Explorer XX topside sounder satellite was spin-stabilized about its major inertia axis at about 1.5 rpm, but experienced in a subsequent loss of spin. The mechanism for this loss of angular momentum has been described[1] in terms of an interaction with the solar radiation field. Originally, the incentive for the investigation was the Canadian Alouette I satellite which is similar in many respects to the Explorer XX.

The theory was formulated in terms of continuous sunlight and it also presumed that the solar vector and the satellite spin vector were perpendicular. The validity of the approach was then established on the basis of the correct shape of the spin history curve predicted by this theory, and the reasonable

Received September 18, 1969.

* Assistant Professor, Institute for Aerospace Studies.
† Graduate Student, Institute for Aerospace Studies.

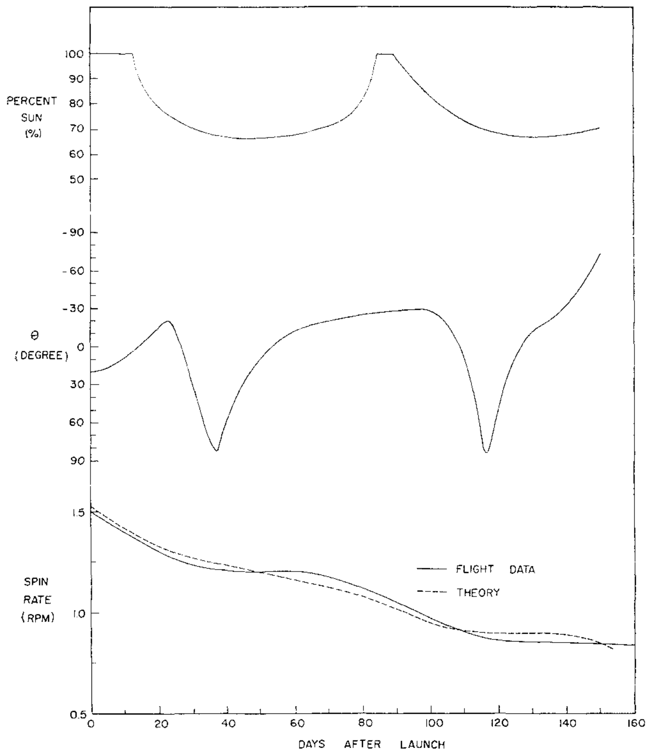

Fig. 1 Sunlight fraction δ (t) and the spin axis attitude $\theta(t)$.

empirical constant required to account for the above two assumptions. A refined analysis[2] was completed subsequently which explicitly incorporates the known histories of the spin axis attitude and percent sunlight. The net torque per satellite rotation due to each antenna boom can be expressed[2] as

$$G(t) = -\frac{pdl^2\delta(t)}{9\pi} \cdot \frac{\omega(t)T}{1 + \omega(t)^2T^2} (2[3\alpha f_1\{\theta(t)\} + 4\beta f_2 \times \{\theta(t)\}]\, S(1) + [4\beta f_3\{\theta(t)\} - 9\alpha f_2\{\theta(t)\}]\, S'''(0)/\lambda(t))$$

where t is the time into flight, p is the solar pressure on a unit area of perfectly absorbing surface normal to the incident radiation, d and l are boom diameter and length, $\delta(t)$ is the fraction of the time spent in the sunlight. The symbols α and β denote the coefficients of absorbtivity and reflectivity of the boom, $\omega(t)$ the satellite spin rate, T the boom thermal time constant, and $\lambda(t) = \rho\omega(t)^2l^4/B$, where ρ and B are the mass density (per unit length) and flexural stiffness of the boom. The spin axis attitude enters via f_1, f_2, and f_3 which are functions of the angle between the spin axis and the solar vector, $\theta(t)$.
Specifically,

$$f_1(\theta) = (1 + \sin^2\theta)E(\cos\theta) - 2\sin^2\theta K(\cos\theta)$$

$$f_2(\theta) = \sin^2\theta[K(\cos\theta) - E(\cos\theta)]$$

$$f_3(\theta) = (1 + \cos^2\theta)E(\cos\theta) - \sin^2\theta K(\cos\theta)$$

where K and E are complete elliptic integrals of the first and second kinds. Finally, the boom shape function $S(\xi)$, $0 \leq \xi \leq 1$, is the solution of the differential equation (a prime denotes differentiation with respect to ξ)

$$2S'''' - \lambda(1 - \xi^2)S'' + 2\lambda\xi S' - 4\lambda S = 0$$

together with the appropriate boundary conditions.

Using this theory, excellent agreement was obtained[2] with the flight data for Alouette I. The purpose of this Note is to communicate similar calculations for the Explorer XX. Figure 1 contains the relevant flight data. The sunlight fraction $\delta(t)$ and the spin axis attitude $\theta(t)$ are shown. The lower part of the figure depicts the observed spin history together with the gratifying similar results of the present theory.

References

[1] Etkin, B. and Hughes, P. C., "Explanation of the Anomalous Spin Behavior of Satellites with Long, Flexible Antennae," *Journal of Spacecraft and Rockets*, Vol. 4, No. 9, Sept. 1967, pp. 1139–1145.

[2] Hughes, P. C. and Cherchas, D. B., "Influence of Solar Radiation on The Spin Behaviour of Satellites with Long Flexible Antennae," *CASI Transactions*, Canadian Aeronautics and Space Institute, Vol. 2, No. 2, Sept. 1969.

Base-Heating Measurements on Apollo Block II Command Module

William K. Lockman*
NASA Ames Research Center, Moffett Field, Calif.

Nomenclature

d	=	maximum model diameter (Fig. 1)
H_t	=	freestream total enthalpy
h_w	=	static enthalpy at model surface
l	=	model length (Fig. 1)
M_∞	=	freestream Mach number
q_b	=	base heat-transfer rate
q_{hem}	=	stagnation-point heat-transfer rate for hemispherical probe
$q_{s_{\alpha=0}}$	=	stagnation-point heat-transfer rate for model at zero angle of attack
R_b	=	base radius of model (Fig. 1)
R_c	=	corner radius of model (Fig. 1)
R_{hem}	=	radius of hemispherical probe
R_n	=	nose radius of model (Fig. 1)
$Re_{\infty,d}$	=	freestream Reynolds number based on maximum model diameter
z	=	radial coordinate in pitch plane of model (Fig. 1)
α	=	angle of attack (Fig. 1)

Introduction

NUMEROUS tunnel tests have previously been made to determine the heating to the conical afterbody of the Apollo command module (see, e.g., Refs. 1–5). However,

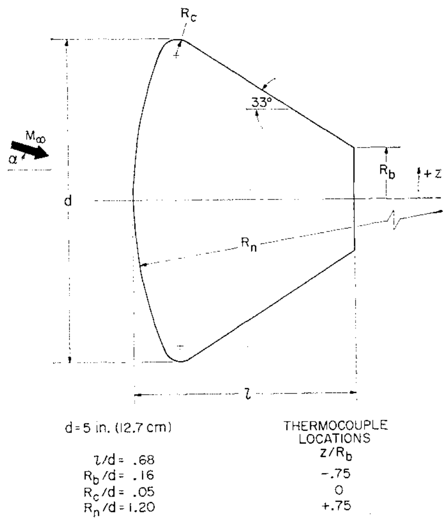

Fig. 1 Apollo Block II model.

Received September 25, 1969.

* Research Scientist. Member AIAA.